Radio OH Observations of the First Interstellar Comet 2I/Borisov from the Arecibo Observatory

Kevin N. Ortiz Ceballos [ID],[1,2] Arianna H. Colón Cesaní [ID],[1,3] Ellen S. Howell,[4] Abel Méndez [ID],[1] Yanga R. Fernández [ID],[5,6]
Amy J. Lovell,[7] Noemi Pinilla-Alonso [ID],[6,8] M. Womack [ID],[5,6] and Génesis M. Ferrer Imbert[1,2]

[1]*Planetary Habitability Laboratory, University of Puerto Rico at Arecibo, P.O. Box 4010, Arecibo, Puerto Rico 00614, USA*
[2]*Department of Physics, University of Puerto Rico, Río Piedras Campus, San Juan, Puerto Rico, USA*
[3]*Department of Physics, University of Puerto Rico, Mayagüez Campus, Puerto Rico, USA*
[4]*Lunar and Planetary Laboratory, University of Arizona, Tucson, AZ, USA*
[5]*Department of Physics, University of Central Florida, FL, USA*
[6]*Florida Space Institute, University of Central Florida, FL, USA*
[7]*Agnes Scott College, Decatur, GA, USA*
[8]*Arecibo Observatory, University of Central Florida, Arecibo, PR, USA*

Draft version as of December 15, 2020.

ABSTRACT

Comet 2I/Borisov was first observed September 8, 2019 and was quickly identified as originating from outside the Solar System due to its highly eccentric, hyperbolic orbit. This is only the second such body that has been detected after 1I/'Oumuamua, which unlike Borisov showed no coma. Radio observations can measure the presence of the hydroxyl (OH) radical, a photodissociation product of water, in the comet's coma, quantifying the comet's activity. We observed interstellar comet 2I/Borisov with the Arecibo Observatory as it passed over its field of view in the fall of 2019. The OH lines were not detected. We find 3σ upper limits to the OH and H_2O production rates of improved precision to previously reported results for September and October 2019, with the lowest limits at $Q_{OH} < 7.403 \times 10^{26}$ mol/s and $Q_{H20} < 6.295 \times 10^{26}$ mol/s for late September. Our results agree with reported ultraviolet, optical and radio observations of 2I/Borisov, which are consistent with low water production. 2I/Borisov did not undergo significant outbursts during the observing period.

Keywords: comets: individual (2I) – comets: general – radio lines: planetary systems

1. INTRODUCTION

Our knowledge of the composition of other planetary systems is limited to what we can study from their direct observation. Though advances in infrared imaging and interferometry have greatly expanded our capabilities for these observations in recent decades, the sheer distance to other stars greatly limits what can be seen with current technology. The detection of interloping interstellar objects which plausibly originate from other planetary systems as they pass through our own Solar System has presented a novel opportunity for studying the composition of these other systems up close. In this study, we report the results of one such opportunity, in which we observed interstellar comet 2I/Borisov

Corresponding author: Kevin Ortiz Ceballos
kevin.ortiz22@upr.edu

with the Arecibo Observatory to search for OH emission and constrain its water production rate.

1I/'Oumuamua was the first interstellar object to be discovered in the Solar System, detected in October 19, 2017 with an open trajectory of eccentricity $e = 1.20$ (Meech et al. 2017a). Despite a perihelion of 0.254 AU, it showed no coma (Meech et al. 2017b), although cometary activity was inferred from observed changes in its orbit that were attributed to mass loss from volatile outgassing (Micheli et al. 2018). Two years after the detection of 1I/'Oumuamua, a second interstellar object was identified traversing the Solar System. 2I/Borisov, initially designated as C/2019 Q4 (Borisov), was discovered on August 30, 2019 (MPEC 2019-R106). Subsequent astrometric measurements were used to model its orbit, which showed it was highly hyperbolic, with an eccentricity of $e = 3.36$ (Guzik et al. 2020). This placed the interstellar object on a greater hyperbolic trajectory than any other comet

or asteroid previously observed, and made evident its origin outside of the Solar System.

2I/Borisov showed cometary activity from its first observations (e.g. de León et al. 2019) and during its passage through the Solar System, despite a perihelion of 2.007 AU, much greater than 'Oumuamua's 0.254 AU. Observations at different wavelengths characterized 2I/Borisov as not easily distinguishable from a standard Solar System comet beyond its hyperbolic orbit. The interstellar object showed a visible, well-defined dust coma (Fitzsimmons et al. 2019; Yang et al. 2020; Zubko et al. 2019), and its elevated abundance ratio of CO/H_2O may provide information about its formation and thermal history (Bodewits et al. 2020). Despite the source of comet 2I/Borisov being unknown, a probable previous stellar encounter with the M-dwarf Ross 573 dating back to approximately one million years ago has been identified (Bailer-Jones et al. 2020).

The primary volatile constituent of Solar System comets is water ice, and thus the gas component of a cometary atmosphere, or coma, has abundant hydroxyl (OH) produced through photodissociation of the H_2O water vapor due to solar radiation (Combi et al. 2004). It is very difficult to detect H_2O from the ground due to its presence in the atmosphere, but if we detect OH, we can then calculate the OH production rate and from it find the comet's H_2O production rate (Crovisier et al. 2002). These rates are designated as Q_{OH} and Q_{H20} respectively.

Obtaining H_2O production rates is important for comet characterization because it allows for analysis of outgassing properties of comet nuclei as well as an evaluation of compositional homogeneities and inhomogeneities of its matter. These rates are also necessary for calculating the presence of other volatiles and their relative concentrations and production. The abundance of Q_{H20} with regards to volatiles gives an overview of the concentration of the various gas productions for most comets (Bockelée-Morvan et al. 2004).

Radio spectroscopy serves as a powerful tool to detect the presence of OH in cometary atmospheres. While near-UV, visible and infrared wavelength observations can detect OH lines (Combi et al. 2004; Crovisier et al. 1997), these observations require very good atmospheric conditions or space telescopes, and can suffer from atmospheric extinction. Furthermore, they may have difficulty fully resolving the OH spectral lines, and are often limited to sampling only small parts of the coma, requiring extrapolation for complete results. Radio observations, on the other hand, can sample a large part of the coma, allowing for more total characterization. They are also rarely affected by weather conditions or atmospheric effects (Crovisier et al. 2002).

To observe OH in the radio spectrum, four principal spectral lines at 1612, 1665, 1667 and 1720 MHz resulting from the 18-cm Λ-doublet transitions can be studied. The intensity

Table 1. Observation conditions for interstellar comet 2I/Borisov

UTC Date and Time	r_H (AU)	$\dot{r}_H$ (km s^{-1})	Δ (AU)	α (deg)
2019-Sep-22 12:15	2.631	-24.412	3.203	16.34
2019-Sep-23 12:15	2.617	-24.239	3.181	16.54
2019-Sep-26 12:00	2.575	-23.700	3.117	17.14
2019-Sep-27 12:00	2.562	-23.514	3.095	17.34
2019-Oct-06 11:30	2.445	-21.679	2.907	19.14
2019-Oct-19 11:30	2.293	-18.469	2.651	21.74
2019-Nov-04 11:00	2.145	-13.540	2.373	24.70
2019-Nov-09 10:45	2.108	-11.780	2.298	25.52

of these spectral lines will depend directly on the heliocentric radial velocity, $\dot{r}_H$, of the comet, meaning that one drawback of radio observations of OH is that these lines will not always be detectable (Schloerb & Gerard 1985).

The Arecibo Observatory 305-m radio telescope has been used successfully many times to detect the 18-cm OH spectral lines from comets (Giguere et al. 1980; Cordes et al. 1990; Lovell et al. 2002; Howell et al. 2007; Lovell & Howell 2015). Though most of these comets have been closer to Earth than 2I/Borisov, the heliocentric radial velocities for 2I/Borisov shown in Table 1 correspond to potentially strong OH lines for this observing period (Despois et al. 1981), increasing the likelihood of a detection.

In this paper, we present the results of an observing campaign carried out with the Arecibo 305-meter radio telescope to detect the 18-cm OH spectral lines from interstellar comet 2I/Borisov. In Section 2, we present the observation methods utilized during the campaign, and Section 3 covers the resulting non-detections of the OH spectra. In Section 4 we discuss our results, calculate upper limits on OH and water production from 2I/Borisov and compare with results from other reported observations.

2. OBSERVATIONS AND DATA REDUCTION

We observed interstellar comet 2I/Borisov on eight occasions in 2019 between September 22 and November 9 until it was no longer visible from Arecibo. The 1612, 1665, 1667 and 1720 MHz OH lines were observed, but results are only reported for the 1667 MHz line since no lines were detected, and it is expected to be strongest (Cordes et al. 1990).

Ephemerides were taken from the Jet Propulsion Laboratory's HORIZONS system, and used to track the comet by adjusting pointing in 5-minute intervals. The single-pixel L-wide receiver was used for all observations. The L-wide average beamwidth for the frequencies observed is of 170".

Observation conditions are listed in Table 1. Heliocentric distance and radial velocity are given by r_H and $\dot{r}_H$ in units of AU and km s^{-1}, respectively. Geocentric distance is given

by Δ in units of AU, and the Sun-target-observer phase angle is given by α in degrees.

Radio frequency interference is not typically a problem for single-line spectral observations with Arecibo, but the broadband data were nonetheless checked to confirm no interference in the frequencies of interest by inspecting the full Stokes images for known interference patterns, and by corroborating with the Observatory's own interference monitoring reports.

Two observational configurations were used. The first one followed the protocol laid out by Howell et al. (2007), which proved effective in observations of 9P/Tempel 1 with Arecibo. The "interim" correlator was used, with which spectra are produced in dual-linear polarizations for the four specific lines investigated. Both polarizations are combined into a single intensity measurement for the results presented here.

The second configuration was implemented using the Mock Spectrometer with a similar protocol to the one used by Gicquel et al. (2014) to detect the OH line in comet 103P/Hartley 2 using the Green Bank Telescope. Spectra were produced in Full Stokes mode; Stokes I was used for this study. The line-of-sight radial velocity of 2I/Borisov was recorded from the JPL ephemerides and used to adjust the expected line location to 0 km s^{-1} cometocentric velocity in the final results. This configuration was not as sensitive as the first approach. The results presented in Figure 1 include data obtained from both configurations, but only data from the "interim" correlator was used for the analysis.

3. RESULTS

The reduced measurements taken with both the "interim" correlator and the Mock spectrometer are presented in Figure 1. Plot (a) in Figure 1 is a full integration over all of the dates in which the comet was observed from Arecibo, and the remaining plots are the integrations of the individual dates. For the full integration, only the "interim" correlator results are presented as these were taken over the full observing period. Spectra are centered on the expected line position as determined from line-of-sight radial velocity of the comet given by the JPL ephemerides. Results from the interim correlator and the Mock spectrometer are presented separately in the red and blue lines respectively, and the 3σ limit for the interim correlator data is given by the dotted horizontal lines. The 3σ limit for the Mock data is in all cases significantly greater. In every case, the interim correlator results give the better constraint on flux, and their 3σ limits are the ones used for finding upper limits.

We did not detect any emission or absorption of OH at the 1667 MHz line in our observations above 3σ. 2I/Borisov was not reported to undergo any significant outbursts during the observing period. With this result, we can establish upper limits on the intensity of any OH spectral line, and its OH and water production rates.

4. DISCUSSION

4.1. *Upper limits on production rates*

Cometary OH spectral lines are often asymmetric, and their shapes are not easily predicted. However, the average flux density over the full linewidth can be predicted with a simpler symmetrical model that is still physically consistent with the gas kinematics of the coma. Schloerb & Gerard (1985) adopt a model of symmetrical radial outflow with this purpose. They obtain an expression for the average flux density of a cometary OH line as:

$$S_\nu = \frac{A_{ul} i k T_{BG}}{4\pi\Delta^2} \frac{c}{2\nu V_{max}} \frac{2F_u + 1}{8}\Gamma \tag{1}$$

Here, A_{ul} is the Einstein spontaneous emission coefficient, which describes the probability per unit time of spontaneous emission in the observed wavelength. i is the inversion, which is given by $i = (n_{uT} - n_{lT})/(n_{uT} + n_{lT})$ with n_{uT} and n_{lT} the total population of OH molecules at the upper and lower level of the Λ-doublet, respectively. This value will be dependent on the comet's heliocentric radial velocity (Combi et al. 2004). k is the Boltzmann constant and T_{BG} is the background sky temperature. Δ is the observer-to-comet distance, and is included in the $1/4\pi\Delta^2$ factor to reduce the total projected flux to the specific flux density as observed by the telescope.

If V_{max} is the maximum expansion velocity of the comet, then $2\nu V_{max}/c$ is the total frequency linewidth at zero intensity (according to the simplified model of symmetrical radial outflow adopted). The inverse of this last term is then factored into the equation for the average flux density to model a simplified, symmetric spectral line.

The $(2F_u + 1)/8$ term gives the fraction of molecules at the specific level of the transition observed, with F_u being the angular momentum quantum number for the transition. And finally, Γ is $\Gamma \equiv Q_p\tau_{OH}$, where Q_p is the production rate of the *parent* molecule of OH and τ_{OH} is the lifetime of OH molecules. There may be other molecules that contribute to the production of OH besides H_2O, and this is accounted for by dealing with a general Q_p. Though there are difficulties in estimating these two values individually, Schloerb & Gerard find that empirical estimates of Γ can be successfully employed.

Tacconi-Garman et al. (1990) use this expression to further approximate the OH production rate from radio observations of the 1667 MHz spectral line specifically. First they identify that $2V_{max}S_\nu = I_{OH}$, the velocity-integrated flux. Then, they take corresponding A_{ul} and F_u values for the 1667 MHz line and assume a cometary background temperature of 3.3K. This leaves the expression for the OH production rate Q_{OH} as:
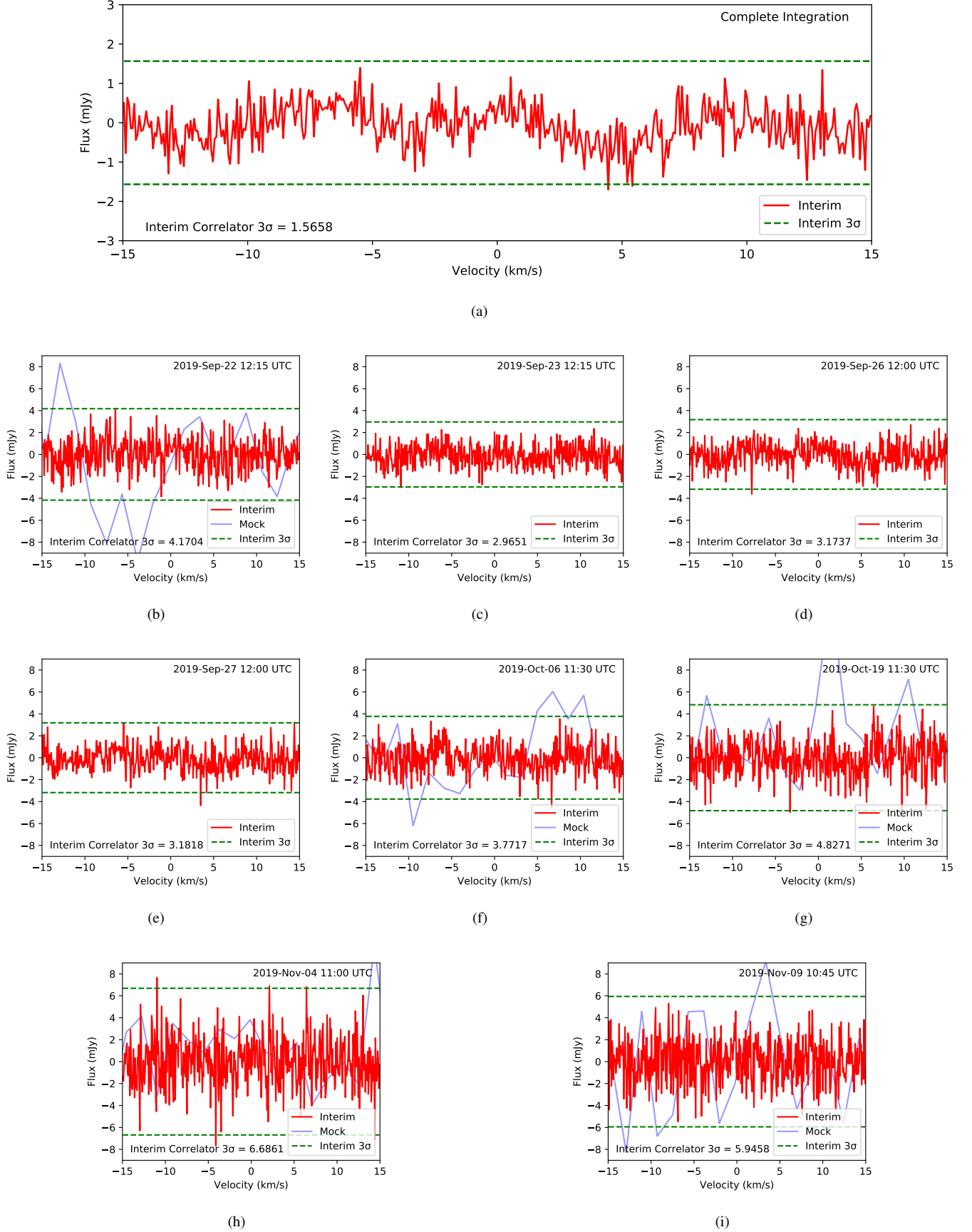
Figure 1. Results from the Arecibo observations of the 1667 MHz OH spectral line in comet 2I/Borisov. (a) shows the full integration over all the dates observed, and (b) to (i) show the integrations for the individual days.

$$Q_{\text{OH}} = \frac{7.06 \times 10^{25}}{i} \times$$
$$\left(\frac{3.3\text{K}}{T_{\text{BG}}}\right)\left(\frac{10^5\text{s}}{\tau_{\text{OH}}}\right)\left(\frac{\Delta}{1\text{AU}}\right)^2 \left(\frac{I_{\text{OH}}}{1\text{ mJy km s}^{-1}}\right)\text{mol s}^{-1} \quad (2)$$

To find the upper limits on Q_{OH}, values for the inversion i are taken from the model of Despois et al. (1981) according to the heliocentric radial velocity of the comet at every observation date (listed in Table 1). Figure 2 shows the inversion model, with the observation dates labeled. It can be seen that most observations occurred at moments of high i, peaking at ~0.5 around the September 27 and October 6 observations. This means that expected line intensity should have been significantly stronger than in other moments for these dates with increased inversion, representing an improved constraint on Q_{OH} and Q_{H2O} from our upper limits.
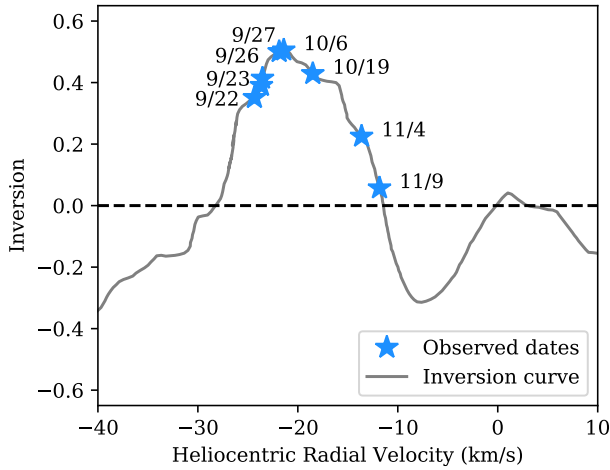

Figure 2. Inversion model from Despois et al. (1981), with each date observed marked along the inversion curve according to the heliocentric radial velocity of the comet.

T_{BG} is taken to be 2.7K. We use the Δ values from Table 1 and assume a standard OH lifetime τ_{OH} of 2×10^5 s (Combi et al. 2004). This last value is scaled by the squared heliocentric distance $r_H{}^2$ in the calculations of Equation 2. We determine I_{OH} from flux upper limits and a 1.6 km/s linewidth, which comes from an assumption of an outflow velocity of 0.8 km/s for the OH parent molecules. We present these values in Table 2, together with estimated upper limits on Q_{OH} found from applying Equation 2.

Finally, to estimate upper limits on the water production rates, we can use the empirical conversion formula:

$$Q_{\text{H}_2\text{O}} = 1.361 \, r_{\text{h}}^{-0.5} \, Q_{\text{OH}} \quad (3)$$

given by Schleicher et al. (1998) for finding the water production rate $Q_{\text{H}_2\text{O}}$ from a known value of Q_{OH}. This relation was

derived from the mean lifetimes, velocities and scale lengths from Cochran & Schleicher (1993). We present the resulting upper limits on $Q_{\text{H}_2\text{O}}$ in Table 2.

4.2. *Comparison with reported observations*

A comparison between our upper limits of the water production rate and other reported results is presented in Figure 3 with respect to their heliocentric distances. The results of Q_{OH} reported by Opitom et al. (2019) and Crovisier et al. (2019) were converted to Q_{H20} using the empirical relation from Schleicher et al. (1998). As shown in the figure, the Arecibo constraints improve on the precision of the results of Opitom et al. (2019) and Crovisier et al. (2019), and are consistent with McKay et al. (2020) and Xing et al. (2020) while reporting several different dates, including the earliest known result for September 22.

Based on optical spectroscopic observations of 2I/Borisov with the 4.2-meter William Herschel Telescope and the ISIS spectrograph, Opitom et al. (2019) reported a 3σ upper limit of OH production of $Q_{\text{OH}} = 2 \times 10^{27}$ molecules s^{-1} on October 2 and 13, 2019 at 2.50 AU and 2.36 AU respectively. The reported Q_{OH} can be converted into $Q_{\text{H}_2\text{O}} = 2.7 \times 10^{27}$ molecules s^{-1} using the empirical relation described in Equation 3, taken from Schleicher et al. (1998).

McKay et al. (2020) observed 2I/Borisov on October 11 2019 with the ARCES instrument on the 3.5-meter ARC Telescope at Apache Point Observatory, finding a water production rate of $(6.3 \pm 1.5) \times 10^{26}$ molecules s^{-1} at 2.38 AU from the sun. This value was derived from optical spectroscopy of a [O I] 6300 °A line emission detection, assuming that $Q_{\text{H}_2\text{O}}$ was its main source.

Crovisier et al. (2019) estimate a tentative production rate for OH of $(3.3 \pm 0.9) \times 10^{27}$ molecules s^{-1} from the 1667 MHz OH line in 2I/Borisov. This value was reported from a marginal detection obtained after fifteen hours of observations with the Nancay Radio Telescope during October 2-25 2019, using the expansion velocity 0.5 km/s for the parent molecules. Using the relation from Equation 3, we can convert this to a water production rate of $(2.9 \pm 0.8) \times 10^{27}$ molecules s^{-1}. As seen in Figure 3, our results imply lower production rates at least for the individual dates of October 6 and 19, 2019.

The ultraviolet observations by Xing et al. (2020) with the *Swift* space telescope constrain the water production rates to a maximum of $(10.7 \pm 1.2) \times 10^{26}$ molecules s^{-1} at perihelion, quickly decreasing to $(4.9 \pm 0.9) \times 10^{26}$ molecules s^{-1} post-perihelion. Their results also agree with previous Yang et al. (2020) reports that indicate a lack of icy grains in the coma, where even if these were present, they would barely contribute to 2I/Borisov's water production rate. The authors also highlight that although the increase in water production rate of 2I/Borisov is at the lower end of the Jupiter-family

Table 2. Upper limits OH lineflux and OH and water production rates for comet 2I/Borisov

UTC Date	r_H (AU)	i	3σ flux limit (mJy)	Max. I_{OH} (mJy km s^{-1})	Max. Q_{OH} (mol/s)	Max. Q_{H20} (mol/s)
2019-Sep-22 12:15	2.631	0.38	4.170	6.673	1.123×10^{27}	9.421×10^{26}
2019-Sep-23 12:15	2.617	0.392	2.965	4.744	7.715×10^{26}	6.490×10^{26}
2019-Sep-26 12:00	2.575	0.424	3.174	5.078	7.571×10^{26}	6.421×10^{26}
2019-Sep-27 12:00	2.562	0.433	3.182	5.091	7.403×10^{26}	6.295×10^{26}
2019-Oct-06 11:30	2.445	0.495	3.772	6.035	7.435×10^{26}	6.472×10^{26}
2019-Oct-19 11:30	2.293	0.452	4.827	7.723	9.854×10^{26}	8.856×10^{26}
2019-Nov-04 11:00	2.145	0.216	6.686	10.698	2.615×10^{27}	2.430×10^{27}
2019-Nov-09 10:45	2.108	0.048	5.946	9.513	1.016×10^{28}	9.526×10^{27}
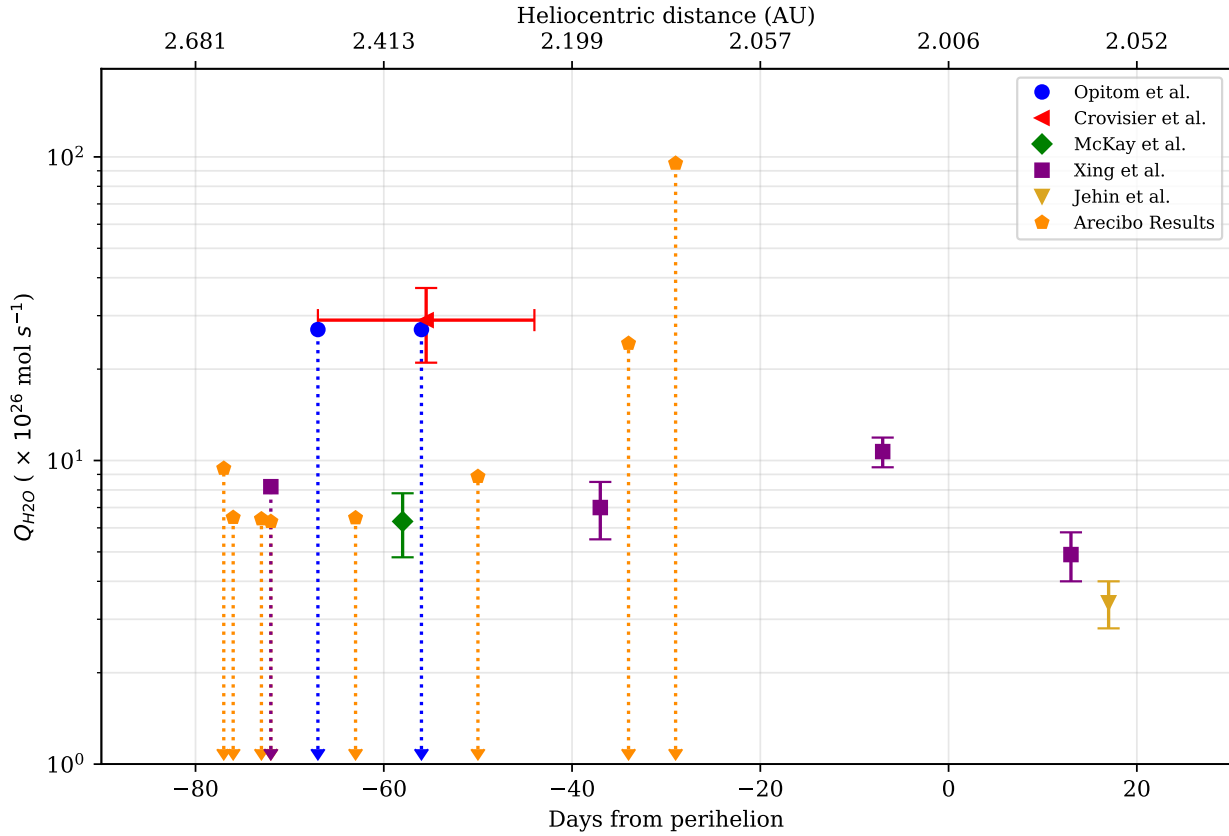
Figure 3. Water production rates of 2I/Borisov over time from various reported observations. Values for Q_{H20} from Opitom et al. (2019) and Crovisier et al. (2019) were produced using their respective results of Q_{OH} and converted by using the empirical relation from Schleicher et al. (1998). Dotted arrow lines indicate upper limits, while solid errorbars indicate values obtained from direct detection of spectral lines.

comets, it increased more rapidly than most dynamically new comets. In addition, 2I/Borisov's power-law exponents of the production rate trend with heliocentric distance were close to those of C/2009 P1 (Garradd) and C/2003 A1. This should imply that the sublimation of icy grains in the coma contributed to the total water production, but since this is not the case with 2I/Borisov, the behavior is most likely caused by seasonal or evolutionary processes.

Jehin et al. (2020) also observed 2I/Borisov post-perihelion in the near-UV, using the 8.2 m Very Large Telescope. OH lines were successfully detected, with a total emission flux of 4.1×10^{-15}erg s^{-1}cm^{-2}. Using the same parameters from Xing et al. (2020), the authors find a water production rate of $Q_{OH} = 3.4 \times 10^{26}$ mol/s.

Mixed results have been reported about 2I/Borisov's chemical composition in relation to other comets in the Solar System. Bannister et al. (2020) detected C_2 and NH_2 in the

interstellar comet and reported that 2I/Borisov is slightly depleted in C_2 at Q(C_2)/Q(CN)=0.61, but rich in NH2, relative to the majority of other Solar System comets at Q(NH$_2$)/Q(CN)=2.7. Their results suggested that the chemical composition of the interstellar object is similar to the broader population of Solar System comets. On the other hand, other significant chemical composition peculiarities of 2I/Borisov are present in its carbon monoxide (CO) and hydrogen cyanide (HCN) ratios. As reported by Cordiner et al. (2020), the HCN to H2O abundance rate is similar to those of previously investigated comets in our Solar System within 2 AU. However, the abundance rate of CO to H2O suggests that the interstellar object likely formed in a carbon monoxide rich environment. Unlike large comets within 2.5 AU of the Solar System, 2I/Borisov's CO to H2O abundances were extremely high and much more elevated than in any other comet in the inner Solar System (Bodewits et al. 2020). Our $Q_{\rm H20}$ upper limits confirm this result. In addition, the CO production rate quickly exceeded the water production rate, as detected by the Ultraviolet-Optical Telescope on the Neil Gehrels Swift observatory (Swift/UVOT) and reported by Bodewits et al. (2020). Though 2I/Borisov behaved like a typical Solar System comet in most aspects other than its trajectory, these two details make it stand out as a comet with a distinct composition, a consequence of its interstellar origin.

5. CONCLUSIONS

The early discovery and identification of 2I/Borisov as an interstellar interloper provided a remarkable opportunity for extended characterization of a small piece of a distant, unknown solar system. We used the Arecibo Observatory's 305-m radio telescope to observe 2I/Borisov for OH emission on eight occasions between September and November 2019. No OH lines were detected and upper limits for the dates observed were determined from the 3σ RMS error on the data, using a simplified model of symmetrical radial outflow for the comet and adopting the expressions of Schloerb & Gerard (1985) and Tacconi-Garman et al. (1990). At the lowest limits found for September 27, 2019, 2I/Borisov's OH and water production rates were of $Q_{\rm OH} < 7.403 \times 10^{26}$ mol/s and $Q_{\rm H20} < 6.295 \times 10^{26}$ mol/s respectively.

Our results are consistent with those published by Opitom et al. (2019), McKay et al. (2020), Xing et al. (2020) and Jehin et al. (2020), which report OH spectral observations at different wavelengths and find OH and water production rates on the order of 10^{26} mol/s, at the same order of magnitude as our upper limits. These results confirm that 2I did not produce water at large amounts during fall 2019.

REFERENCES

Astropy Collaboration, Robitaille, T. P., Tollerud, E. J., et al. 2013, A&A, 558, A33. doi:10.1051/0004-6361/201322068

Bailer-Jones, C. A. L., Farnocchia, D., Ye, Q., et al. 2020, A&A, 634, A14. doi:10.1051/0004-6361/201937231

Bannister, M. T., Opitom, C., Fitzsimmons, A., et al. 2020, arXiv:2001.11605

Bockelée-Morvan, D., Crovisier, J., Mumma, M. J., et al. 2004, Comets II, 391

Bodewits, D., Noonan, J. W., Feldman, P. D., et al. 2020, Nature Astronomy, 4, 867. doi:10.1038/s41550-020-1095-2

Cochran, A. L. & Schleicher, D. G. 1993, Icarus, 105, 235

Combi, M. R., Harris, W. M., & Smyth, W. H. 2004, Comets II, 523

Cordes, J. M., Falchi, A., Lewis, B. M., et al. 1990, AJ, 100, 1655. doi:10.1086/115625

Cordiner, M. A., Milam, S. N., Biver, N., et al. 2020, Nature Astronomy, 4, 861. doi:10.1038/s41550-020-1087-2

Crovisier, J., Leech, K., Bockelee-Morvan, D., et al. 1997, Science, 275, 1904. doi:10.1126/science.275.5308.1904

Crovisier, J., Colom, P., Gérard, E., et al. 2002, A&A, 393, 1053

Crovisier, J., Colom, P., B. N., & Bockelée-Morvan, D. 2019, CBET 4691, International Astronomical Union. http://www.cbat.eps.harvard.edu/iau/cbet/004600/CBET004691.txt

Ćuk, M. 2018, ApJL, 852, L15

de León, J., Licandro, J., Serra-Ricart, M., et al. 2019, Research Notes of the American Astronomical Society, 3, 131

Despois, D., Gerard, E., Crovisier, J., et al. 1981, A&A, 99, 320

Dybczyński, P. A. & Królikowska, M. 2018, A&A, 610, L11

Feng, F. & Jones, H. R. A. 2018, ApJL, 852, L27

Fitzsimmons, A., Hainaut, O., Meech, K. J., et al. 2019, ApJL, 885, L9

Harris, C. R., Jarrod Millman, K., van der Walt, S. J., et al. 2020, Nature, 585, 357

Howell, E. S., Lovell, A. J., Butler, B., et al. 2007, Icarus, 187, 228

Hunter, J. D. 2007, Computing in Science and Engineering, 9, 90. doi:10.1109/MCSE.2007.55

Jehin, E., Manfroid, J., & Hutsemekers, D. 2020, CBET 4719, International Astronomical Union. http://www.cbat.eps.harvard.edu/iau/cbet/004700/CBET004719.txt

Gaidos, E., Williams, J., & Kraus, A. 2017, Research Notes of the American Astronomical Society, 1, 13

Gicquel, A., Milam, S. N., Villanueva, G. L., et al. 2014, ApJ, 794, 1

Giguere, P. T., Huebner, W. F., & Bania, T. M. 1980, AJ, 85, 1276. doi:10.1086/112797

Guzik, P., Drahus, M., Rusek, K., et al. 2020, Nature Astronomy, 4, 53

Kral, Q., Wyatt, M. C., Triaud, A. H. M. J., et al. 2018, MNRAS, 479, 2649. doi:10.1093/mnras/sty1677

Lovell, A. J., Howell, E. S., Schloerb, F. P., et al. 2002, Asteroids, Comets, and Meteors: ACM 2002, 500, 681

Lovell, A. J. & Howell, E. S. 2015, AAS/Division for Planetary Sciences Meeting Abstracts #47

McKay, A. J., Cochran, A. L., Dello Russo, N., et al. 2020, ApJL, 889, L10

Meech, K., Bacci, P., Maestripieri, M., et al. 2017, Minor Planet Electronic Circulars, 2017-U183

Meech, K. J., Weryk, R., Micheli, M., et al. 2017, Nature, 552, 378

Micheli, M., Farnocchia, D., Meech, K. J., et al. 2018, Nature, 559, 223

Opitom, C., Fitzsimmons, A., Jehin, E., et al. 2019, A&A, 631, L8

Ortiz Ceballos, K., Howell, E. S., Méndez, A., et al. 2020, 51st Lunar and Planetary Science Conference, LPI Contribution No. 2326, 2020, id.3078

Pandas development team 2020, Zenodo. doi:10.5281/zenodo.3509134

Portegies Zwart, S., Torres, S., Pelupessy, I., et al. 2018, MNRAS, 479, L17

Schleicher, D. G. 1983, Ph.D. Thesis

Schleicher, D. G. & A'Hearn, M. F. 1988, ApJ, 331, 1058. doi:10.1086/166622

Schleicher, D. G., Millis, R. L., & Birch, P. V. 1998, Icarus, 132, 397. doi:10.1006/icar.1997.5902

Schloerb, F. P. & Gerard, E. 1985, AJ, 90, 1117

Tacconi-Garman, L. E., Schloerb, F. P., & Claussen, M. J. 1990, ApJ, 364, 672

Virtanen, P., Gommers, R., Oliphant, T. E., et al. 2020, Nature Methods, 17, 261. doi:10.1038/s41592-019-0686-2

Xing, Z., Bodewits, D., Noonan, J., et al. 2020, ApJL, 893, L48

Yang, B., Kelley, M. S. P., Meech, K. J., et al. 2020, A&A, 634, L6

Zhang, Q. 2018, ApJL, 852, L13

Zubko, E., Chornaya, E., Videen, G., et al. 2019, Research Notes of the American Astronomical Society, 3, 138

Zuluaga, J. I., Sánchez-Hernández, O., Sucerquia, M., et al. 2018, AJ, 155, 236